Supporting Information

Mechanism in Supported Ru_3Sn_7 Nanoclusters Catalyzed Selective Hydrogenation of Coconut Oil to Fatty Alcohols

Zhicheng Luo[1a], Qiming Bing[1b], Jiechen Kong[a], Jing-yao Liu [b*], Chen Zhao [a*]

[a] Shanghai Key Laboratory of Green Chemistry and Chemical Processes, School of Chemistry and Molecular Engineering, East China Normal University, Shanghai, 200062, China

E-mail: czhao@chem.ecnu.edu.cn (C. Zhao)

[b] Laboratory of Theoretical and Computational Chemistry, Institute of Theoretical Chemistry, Jilin University, Changchun 130023, China.

Email: ljy121@jlu.edu.cn (J. Liu)

[1] Two authors contribute equally to the work

Experimental Section

Chemicals

Coconut Oil (Sinopharm, AR), *n*-dodecane (Sinopharm, > 98% GC assay), Stearic acids (Sinopharm, AR), Stearyl alcohol (Sinopharm, CP), Palmitic acid (Sinopharm, AR), Myristic acid (Sinopharm, CP, >98%), Lauric acid (Sinopharm, >99%), Butyric acid (Sinopharm, >99.5%), Propionic acid (Sinopharm, AR), SiO_2 (Shanghai maikun Co.), $Pd(NO_3)_2$ (J&K, AR), $SnCl_4{\cdot}5H_2O$ (Sinopharm, AR), $Co(NO_3)_2\,6H_2O$ (Sinopharm, AR), $Ni(NO_3)_2{\cdot}6H_2O$ (Sinopharm, AR), $RuCl_3{\cdot}3H_2O$ (J&K, AR), $PtCl_4$ (J&K, AR), Air, H_2 and N_2 gases (99.999 vol.%) were supplied by Shanghai Pujiang Specialty Gases Co., Ltd.

Computational Methods

First-principles spin-polarized density functional theory (DFT) calculations were performed using the Vienna ab initio Simulation Package (VASP) [1]. The projector augmented wave (PAW) method [2, 3] was adopted to describe the electron-ion interactions, and generalized gradient approximation with the Perdew-Burke-Ernzerhof approach (GGA-PBE) [4] was applied to describe the nonlocal exchange correlation energy. An energy cutoff of 400 eV was used in all calculations.

The optimized bulk geometries of Ru_2Sn_3 and Ru_3Sn_7 alloys were calculated based on the experimental crystal structure data [5, 6]. For structure optimization, the Brillouin zone was sampled using (5×5×5) Monkhorst-Pack (MP) k-points grid. The structures were fully relaxed with respect to the lattice constants and atomic positions until the forces exerted on each atom converged to 0.01 eV/Å. The optimized structures of Ru_2Sn_3 and Ru_3Sn_7 alloys were in good agreement with the experimental results for the differences of lattice constants being less than 1%. The (1×1) slab models of (100), (110) and (111) crystal surfaces of Ru_3Sn_7 with the thickness of five atom layers were built based on the optimized Ru_3Sn_7 bulk structure. In surface optimizations, the MP k-points grid was sampled as (5×5×1) with the same convergence criterions of the bulk calculations. A vacuum region of 15Å was employed along the perpendicular direction of the surfaces to avoid the interactions

between the periodic images. The transition states (TS) were located with the climbing-image nudged elastic band (CI-NEB) method and were confirmed by the vibrational analysis. The adsorption energy (E_{ads}) was defined as:

$$E_{ads} = E_{adsorbate\text{-}surface} - E_{surface} - E_{adsorbate}$$

wherein $E_{adsorbate}$, $E_{surface}$, and $E_{adsorbate\text{-}surface}$ represent the total energy of the adsorbate in gas phase, the surface model, and the surface with the adsorbate, respectively. The interaction energy (denoted as E_{inter}), which was defined as the difference between the energies of the coadsorbed structure and the infinite separation state, was also considered.

The formation energies (E_{form}) of Ru_1Sn_2, Ru_2Sn_3 and Ru_3Sn_7 alloys were calculated using the following formula:

$$E_{form} = E_{RuSn} - CE_{Ru} - (1 - C)E_{Sn}$$

where E_{RuSn} is the energy per atom of Ru-Sn alloy bulk unit cell, $E_{Ru}$and E_{Sn} are the energies per atom of pure metallic Ru and Sn bulk unit cell, C and $(1-C)$ are the atom percentages of Ru and Sn in the alloy, respectively. According to this formula, the alloy with lower E_{form} value is more stable and preferred to form.

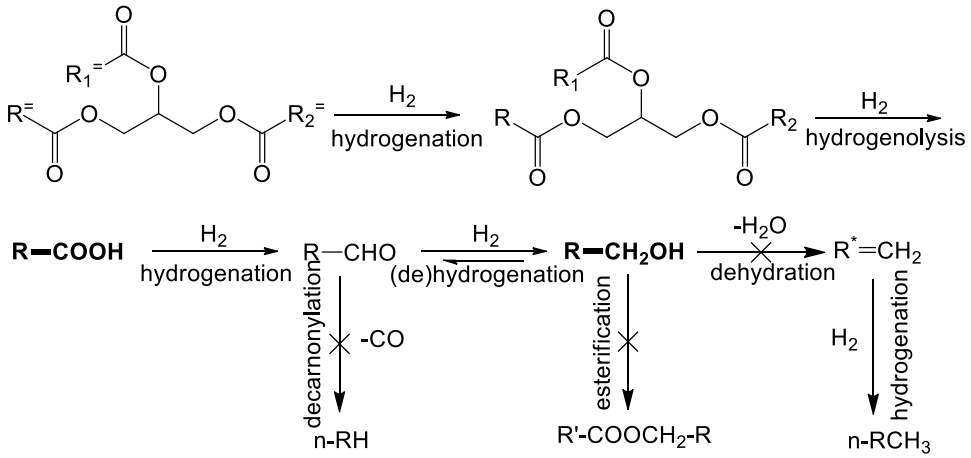

Figure S1. The reaction sequences for selective conversion of coconut oil to fatty alcohols.

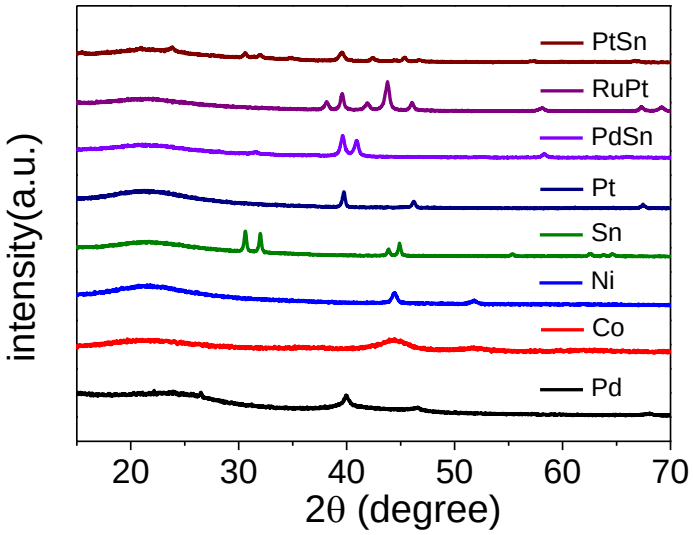

Figure S2. The XRD patterns of the supported metal catalysts on SiO_2 (metal loading: 5 wt%).

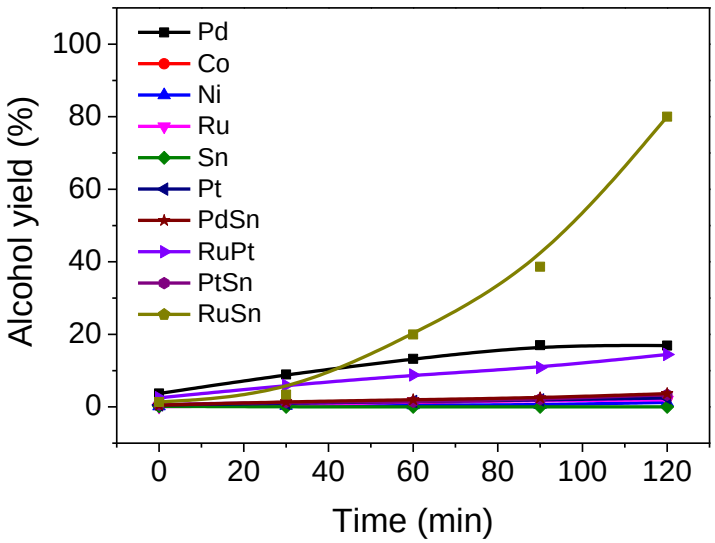

Figure S3. Kinetics curves of stearyl alcohol yields from stearic acid hydrogenation over different metal catalysts. Reaction conditions: Stearic acid (1.0 g), 5% M/SiO_2 (0.2 g), dodecane (80 mL), 240 ˚C, 4 MPa H_2, stirring at 700 rpm.

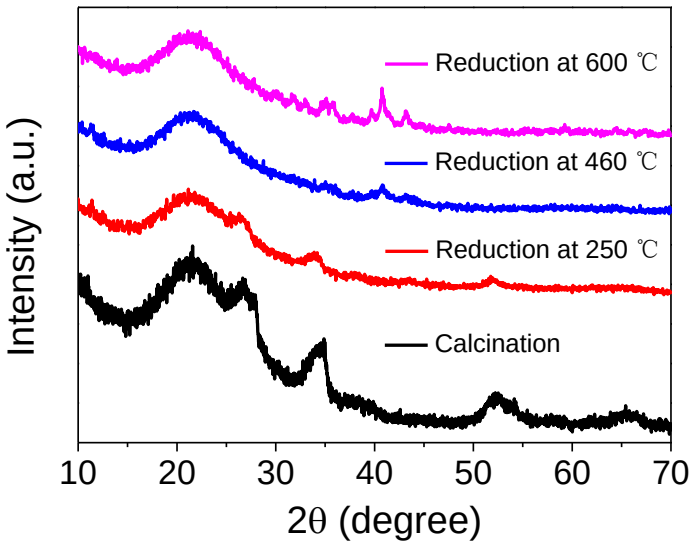

Figure S4. The XRD patterns of 1.5%Ru-4.5%Sn/SiO_2 catalysts prepared at different reduction temperatures.

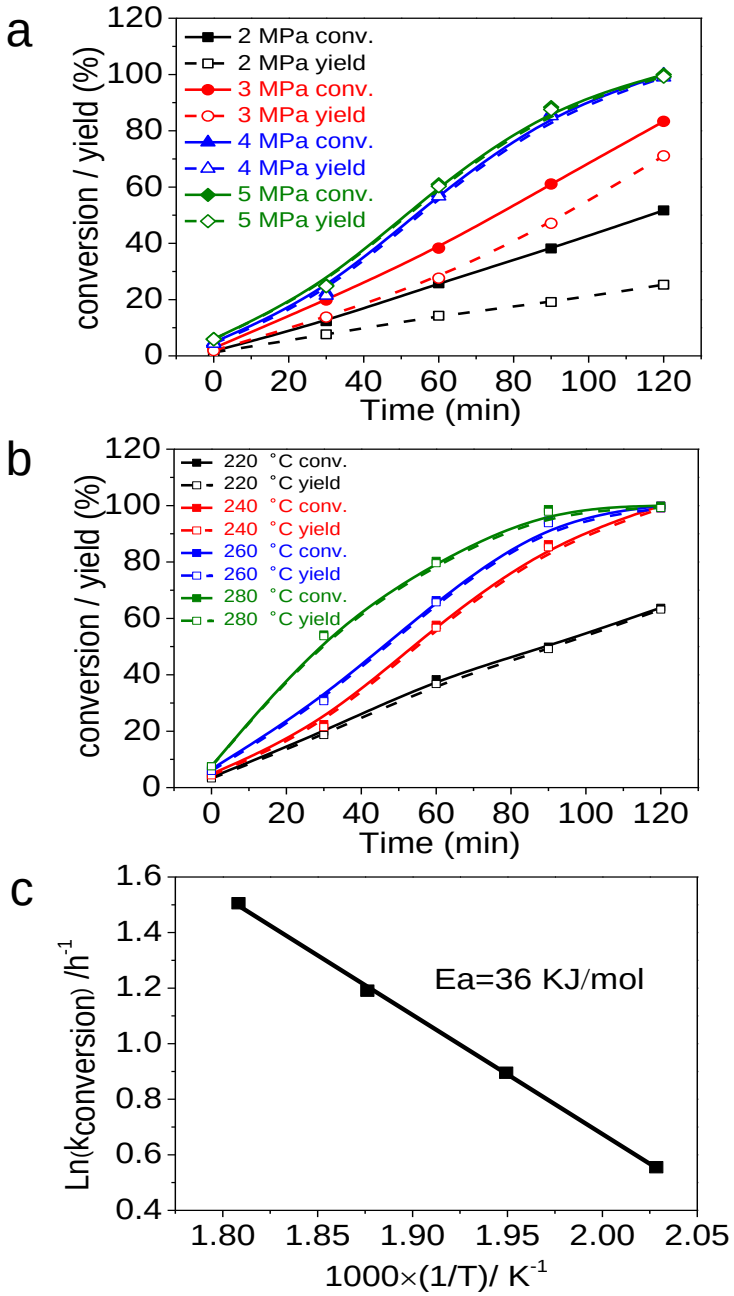

Figure S5. (a) Temperatures and (b) hydrogen pressures impact towards stearic acid conversion and product distributions. Reaction conditions: Stearic acid (1.0 g), catalyst (0.2 g), dodecane (80 mL), 240 ˚C, 4 MPa H_2, stirring at 700 rpm.

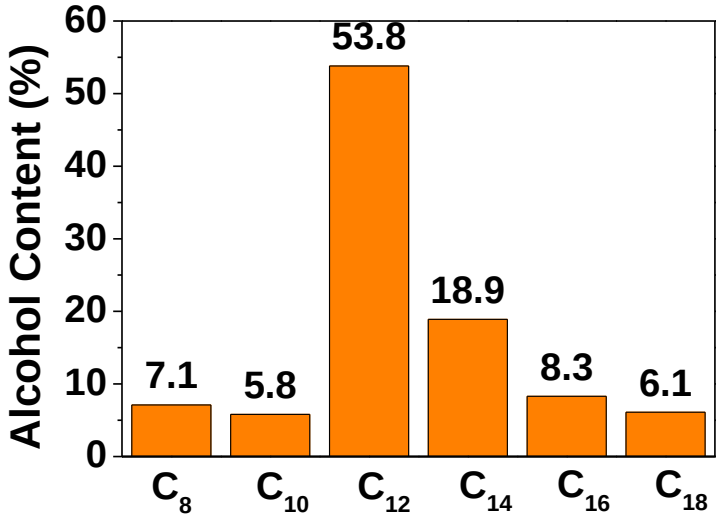

Figure S6. The fatty acid compositions in coconut oil raw material detected by transesterification with methanol. Reaction conditions: coconut oil (1.0 g), CaO (1 g), methanol (100 mL), 80 ˚C, 2 h.

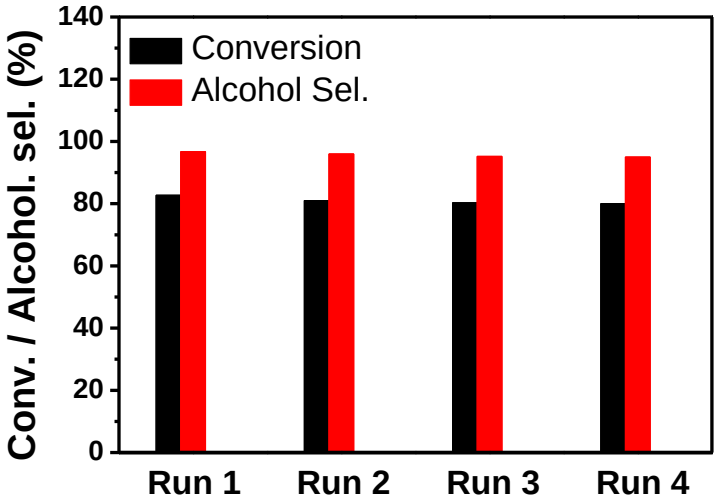

Figure S7. Coconut oil hydrogenation was tested on Ru_3Sn_7/SiO_2 catalyst by four consecutive runs. Reaction conditions: Coconut oil (1.0 g), catalyst (0.2 g), dodecane (80 mL), 240 ˚C, 4 MPa H_2, stirring at 700 rpm.

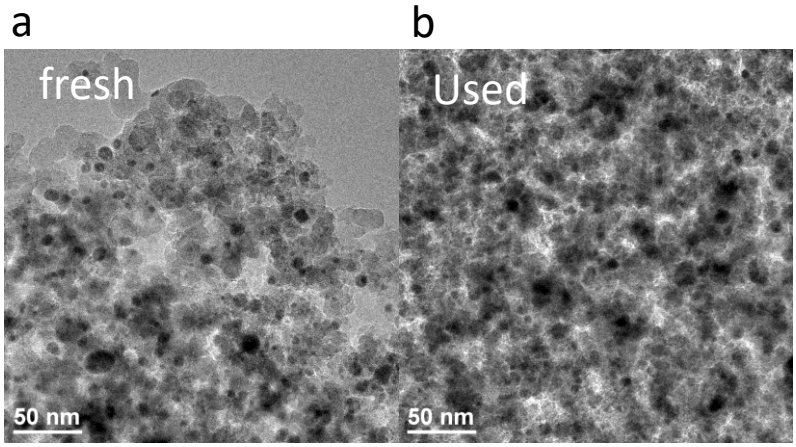

Figure S8. The TEM images of (a) fresh and (b) used Ru_3Sn_7/SiO_2 catalyst.

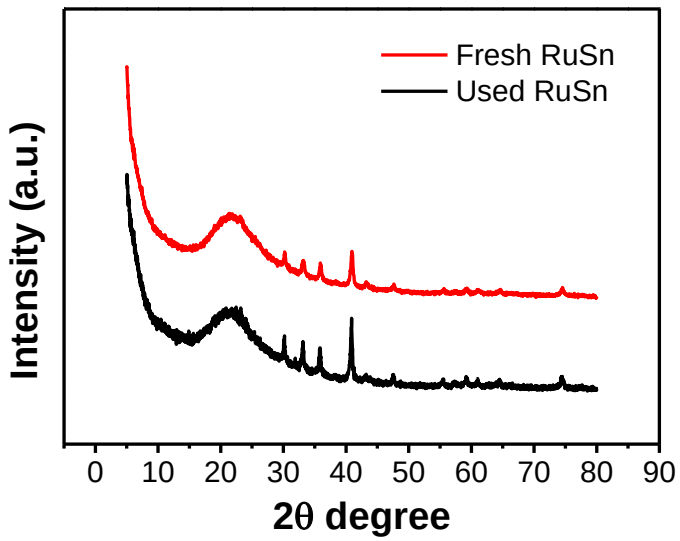

Figure S9. The XRD patterns of fresh and used Ru_3Sn_7/SiO_2 catalyst.

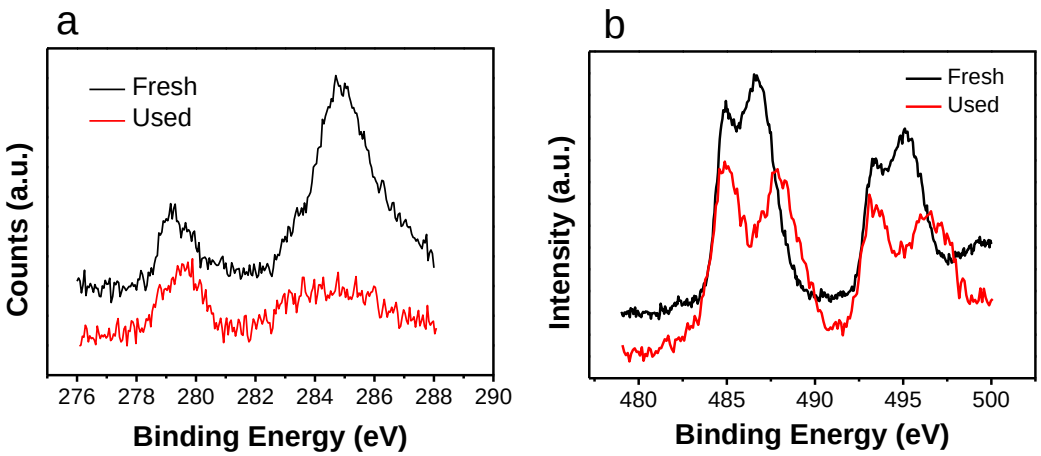

Figure S10. The XPS spectra of fresh and used Ru_3Sn_7/SiO_2 catalyst, (a) Ru $3d_{5/2}$; (b) Sn $3d_{5/2}$.

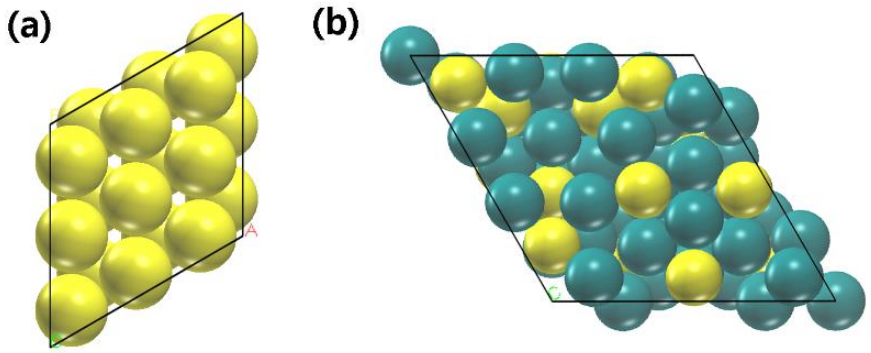

Figure S11. Optimized structure schemes of (a) Ru (0001) (b) Ru_3Sn_7 (111) surfaces. Color scheme: yellow: Ru and cyan: Sn.

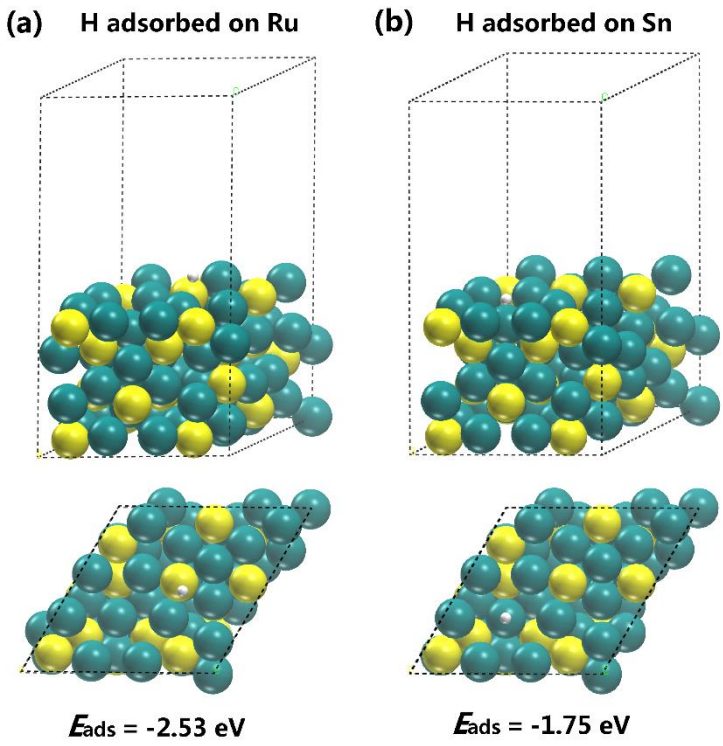

Figure S12. Most stable adosption structures and adsorption energies of H* species at the (a) Ru and (b) Sn site on Ru_3Sn_7 (111) surfaces. Color scheme: yellow: Ru, cyan: Sn, and white: H.

Table S1. The Ru and Sn species information on various $RuSn/SiO_2$ catalysts detected by XPS.

Metal loading (wt%)	BE(eV)		Bulk atomic compositions	Surface atomic compositions
	Ru 3d5/2	Sn 3d5/2	Ru/Sn	$Sn^0/Sn^{\delta+}$
Ru(1.5)	280.2 (Ru^0)		+∞	0
Sn(4.0)		484.9 (Sn^0) 486.9 (SnO)	0	0.1172
Ru(1.5) Sn(1.5)	279.8 (Ru^0)	485.3 (Sn^0) 486.9 (SnO)	0.85	0.3825
Ru(1.5) Sn(3.0)	279.7 (Ru^0)	485.2 (Sn^0) 486.9 (SnO)	0.43	0.3817
Ru(1.5) Sn(4.0)	279.4 (Ru^0)	485.1 (Sn^0) 486.9 (SnO)	0.32	0.7991
Ru(1.5) Sn(6.0)	279.3 (Ru^0)	485.1 (Sn^0) 486.9 (SnO)	0.21	0.2211
Ru(1.5) Sn(7.5)	279.2 (Ru^0)	485.1 (Sn^0) 486.9 (SnO)	0.17	0.2667
Ru(1.5) Sn(9.5)	279.1 (Ru^0)	485.0 (Sn^0) 486.9 (SnO)	0.13	0.1431

Notes and references

1 G. Kresse, J. Furthmuller, *Phys. Rev. B*., 1996, **54**, 11169-11186.
2 P. E. Blochl, *Phys. Rev. B*. 1994, **50**, 17953-17979.
3 G. Kresse, D. Joubert, *Phys. Rev. B*. 1999, **59,** 1758-1775.
4 J. P. Perdew, K. Burke, M. Ernzerhof, *Phys. Rev. Lett*. 1996, **77**, 3865-3868.
5 O. Schwomma, H. Nowotny, A. Wittmann, *Monatsh Chem*. 1964, **95**, 1538-1543.
6 E. Lars, L. Johanna, *Acta Cryst.* 2001, **57**, 85-86.